

Experiments on the transient freezing of water in an inclined rectangular cavity

W. Z. Cao and D. Poulikakos

Mechanical Engineering Department, University of Illinois at Chicago, Chicago, IL, USA

An experimental study was conducted on the transient solidification of water in a rectangular inclined cavity. The dependence of the phase-change interface and of the volume of ice produced on time and on the inclination angle were determined. Characteristic temperature distributions in the cavity were obtained and compared to the predictions of a simple model that neglected the presence of buoyancy-driven flow in the system. Flow visualization in the liquid phase using the laser-sheet technique showed the presence of a bicellular structure. The ice nucleation time at the cold surface exhibited a maximum at an inclination angle of about 60°. An engineering correlation is also reported for the dependence of the volume of ice formed in the system on the inclination angle and on time.

Keywords: water solidification; inclined enclosure

Introduction

The process of freezing of water is common in many engineering applications as well as in nature. When temperature gradients exist in the liquid phase during a solidification process, they initiate a buoyancy-driven flow that may significantly affect the shape of the ice/water interface as well as the progress of the solidification phenomenon.^{1,2} In the following paragraphs, representative studies of phase-change problems in rectangular spaces are discussed. It is worth mentioning in advance that only a few of these studies use water as the working fluid. It appears that waxes (such as paraffin), which, unlike water, do not possess a density extremum at 4°C, are the most popular working substances in solidification studies, since they are easy to handle and their melting/freezing temperature is considerably higher than that of water. Water has been used more often as the working substance in solidification studies around or inside cylinders. Even though these studies are not directly related to the present work, a few key results will be reviewed for the sake of completeness.

Borger and Westwater² measured interface velocities and temperature profiles during the freezing of water and the melting of ice in a rectangular chamber with adiabatic vertical walls and heated or cooled horizontal walls. At the highest Rayleigh number studied, oscillations in the interface velocity were reported. Diaz and Viskanta³ visualized the solid-liquid interface in a layer of n-octadecane heated from below. The effect of initial subcooling was found only to delay the development of the interface morphology. Hale and Viskanta⁴ determined the solid-liquid interface motion during the freezing and melting from above and below of several different substances (not including water) in a rectangular test cell suitable for photographic observations. Flow visualization experiments on the freezing from above⁵ and the melting from below⁶ of n-octadecane provided information on the buoyancy-driven flow in the liquid phase and its effect on the shape of the interface.

Ho and Viskanta⁷ reported basic solid-liquid interface data during the phase change of n-octadecane in a two-dimensional

(2-D) rectangular cavity with conducting vertical walls. The heating or cooling of the cavity was accomplished through the bottom wall. They concluded that for solid-liquid phase-change heat transfer, short extended surfaces are more effective than longer ones. The study of melting of PCM in an inclined rectangular enclosure (an incline between 0° and 60° from the vertical) yielded a correlation for the effect of inclination angle on the time variation of the melt fraction.⁸ Interferometric observations of natural convection during freezing from a vertical flat plate were published by Van Buren and Viskanta.⁹

Jany and Bejan¹⁰ identified the basic scales and regimes of the phenomenon of melting with natural convection in an enclosure heated from the side. With the help of scale analysis, they showed that the phenomenon consists of four regimes: pure conduction, mixed conduction-convection, convection, and "shrinking solid."

Water was used by Cheng et al.¹¹ as the working fluid to investigate the effect of natural convection on ice formation around an isothermally cooled horizontal cylinder. The stagnation point Nusselt number, the local heat transfer coefficient, and the average Nusselt number behavior at the ice/water interface were studied. Flow inversions caused by the presence of the density extension of water at 4°C seriously affected the heat transfer at the ice/water front as well as the development of this front. Gilpin¹² investigated the freezing of water inside a horizontal cylindrical pipe. He predicted theoretically the existence of three quasi-steady modes of convection for some temperatures in the vicinity of 4°C. He observed experimentally reversals of the flow pattern attributed to the existence of the density extremum. These flow reversals involved a transition from one quasi-steady mode to another. Dendritic ice formation was reported by Gilpin¹³ during the freezing of supercooled water in a cylindrical pipe. Herman et al.¹⁴ investigated experimentally the freezing of superheated water around an isothermal horizontal cylinder. Natural convection, affected by the presence of the density extremum of water at 4°C, produced nonuniform ice growth. Bernard-Goertler instabilities resulted in secondary flows that produced waviness at the ice/water interface along the cylinder axis.

The present study deals with the problem of water solidification in an inclined rectangular enclosure with one cooled wall and four insulated walls. The whole range of inclination angles with respect to the gravity vector is examined (0°–180°).

Address reprint requests to Dr. Poulikakos at the Mechanical Engineering Department, University of Illinois at Chicago, P.O. Box 4348, Chicago, IL 60680, USA.

Received 30 April 1990; accepted 29 October 1990

The motivation behind this study is threefold. First, since water abandons in nature, solidification of water occurs in many engineering and geophysical applications, exemplified by heat exchangers of various types, ice storage systems, food freezing, ice production machines, and the freezing of water bodies in our environment. Therefore, studying the fundamentals of the process of freezing of water is well worthwhile. Second, because of the presence of the density extremum of water at 4°C, the results of studies on the solidification of waxes cannot be generalized to predict accurately the behavior of a freezing water body. Third, unlike solidification of water inside or around cylinders,¹¹⁻¹⁴ published studies on the solidification of water in rectangular cavities (a basic geometry from the study of which one may gain valuable experience in predicting the behavior of more complex geometries) are scarce indeed.² Moreover, the effect of the inclination angle of the enclosure with respect to the gravity vector on the process of water freezing has not, to the best of our knowledge, been studied.

In the context of this article, key results on the flow field, temperature field, ice-water interface, and ice volume production are presented and their dependence on the inclination angle and on time is discussed.

Experimental apparatus and procedure

The experimental apparatus consisted of a test section and two supporting devices. The two supporting devices were a data acquisition system and a bath refrigerator circulator.

The test section was a rectangular cavity with two circular tracks attached to it. The tracks were used to rotate the cavity at any desirable angle (Figure 1). The internal dimensions of the water space measured 5.1 cm long by 5.1 cm tall by 5.7 cm deep. The cold wall of the apparatus was constructed out of stainless steel of thickness 0.685 cm. This wall was machined to allow for five thermocouples and a counterflow heat exchanger. The heat exchanger was constructed by milling four channels into the stainless steel surface. The direction of flow of the coolant in the heat exchanger was alternated between adjacent channels to establish isothermally of the wall. Indeed, the stainless steel wall of the apparatus was isothermal within 0.5°C for all the experiments. The coolant was a 50% water/ethylene glycol solution precooled by a bath circulator refrigerator.

The remaining walls of the apparatus were constructed out of Plexiglas of thickness 0.685 cm. To allow for observation and photographing, the front and back walls were made out of a "double" sheet of Plexiglas with a vacuum gap in between (Figure 1). This eliminated condensation on these walls and served as insulation between the water space and the environment. An additional 2-cm-thick styrofoam insulation surrounded the apparatus and helped to practically eliminate heat losses.

A thermocouple column consisting of nine thermocouples was placed at the center of the cavity perpendicular to the cold wall (Figure 1). This thermocouple column yielded information on the evolution of the temperature distribution.

The procedure for the collection of the experimental data is as follows. The cavity is filled with water and positioned at a desired angle with respect to the gravity vector. The coolant in the refrigerator, which is precooled and kept at -25°C throughout the experiments, is suddenly circulated through the heat exchanger machined into the stainless steel wall of the apparatus. As a result, natural convection and eventually solidification takes place inside the cavity. The solid/liquid interface is observed and photographed at approximate time

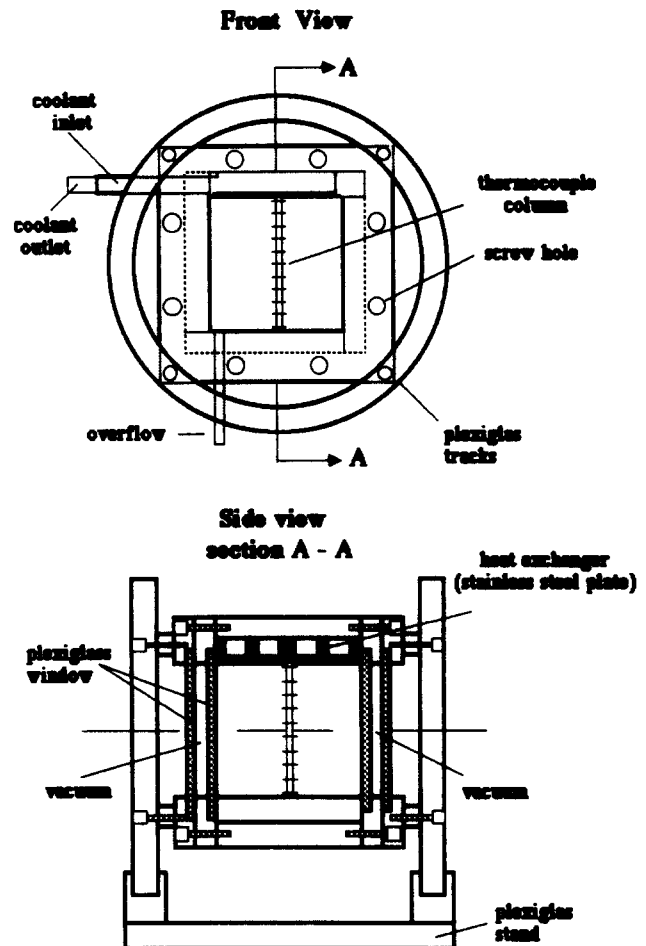


Figure 1 Front view and side view of the test section

Notation

C_p	Specific heat, J/(kg°K)
H	Height of the cavity
L	Latent heat of fusion
T	Temperature
T_c	Cold-wall temperature (°C)
T_i	Initial solution temperature (°C)
T_0	Melting temperature of pure ice (°C)
t	Time
t_n	Ice nucleation time

V	Ice volume
V_T	Total volume of the cavity
V^*	Dimensionless ice volume (Equation 1)

Greek symbols

α	Thermal diffusivity
τ	Dimensionless time (Equation 2)

Subscripts

n	Ice nucleation
s	Solid region

intervals. Temperature measurements are recorded at time intervals that range from 2 seconds at early times to 5 minutes at late times.

The accuracy of the temperature measurements was estimated to be within 3% and was dictated by the accuracy of the software that converted the voltage measurements to temperature measurements. The accuracy of the measurements of the ice volume was estimated to be 8%.

Flow visualization was attempted by using the laser-sheet technique.¹⁵ A rheoscopic suspension of microscopic crystalline disks was added to the fluid and a vertical sheet of laser light, perpendicular to the cold wall, was passed through the test section. The disks are neutrally buoyant and thus have a very large settling time. The concentration of the rheoscopic suspension was 0.1%. The laser sheet was created by passing the beam of a five mW helium–neon laser through a cylindrical lens. Light reflecting off the crystalline disks enabled us to clearly see the general flow pattern within the cavity. Time-exposure photographs were taken of the flow patterns using a Nikon FE 35-mm camera with T-max ASA 400 black and white film. Even though observing the flow was always possible, photographing the flow was not. A discussion of the observed flow field is contained in the following section.

Results and discussion

The temperature variation of the cold wall of the cavity with time for a host of values of the inclination angle is shown in Figure 2. More specifically, Figure 2a presents data for the temperature after ice has formed on the wall surface, i.e., for time longer than the ice nucleation time. These data are taken every 5 minutes for all inclination angles of interest and prove that, for a specific angle, after the ice nucleation time the wall temperature decreases monotonically until it reaches practically a plateau value at about -19°C . The effect of inclination angle is not significant, especially at large time values.

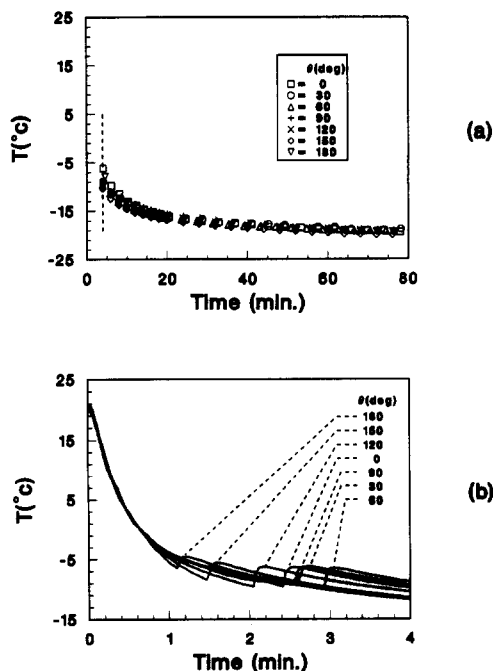


Figure 2 The variation of the cold-wall temperature with time: (a) temperature after the ice formation, (b) temperature before the ice formation

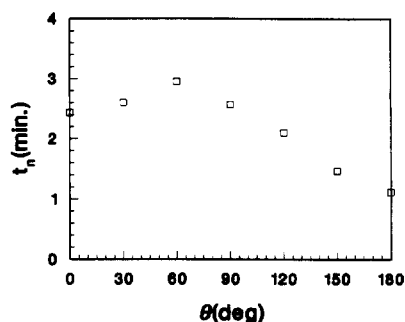


Figure 3 The dependence of the ice nucleation time on the inclination angle

To study the effect of ice nucleation on the wall temperature, data were collected at a fast rate (every 2 seconds) at very early times ($0 < t < 4$ min). Note that in no experimental run the ice nucleation time was greater than 3 minutes. The temperature for the time domain to the left of the dashed line in Figure 2a is reported in Figure 2b using a larger time scale in the abscissa. Clearly, for all inclination angles, the ice nucleation (formation) time is marked by a jump (increase) in the temperature *versus* time curve. This temperature jump is caused by the latent heat of fusion released during the ice formation as well as by the fact that the ice/water interface is at 0°C , which is higher than the pipe wall temperature right before ice is formed. Note, for example, that because of the presence of the buoyancy-driven flow, the pipe wall is subcooled to about -9°C right before ice is formed for $\theta = 120^{\circ}$.

The dependence of the ice nucleation time on the inclination angle is reported in Figure 3. Clearly, t_n does not vary monotonically with θ , and it reaches a maximum at $\theta \approx 60^{\circ}$. Ice forms the fastest on the pipe surface when $\theta = 180^{\circ}$ and the natural convection flow in the liquid phase is the weakest. The physical explanation for why the nucleation time depends on the inclination angle is as follows. It is well known that the nucleation time depends on the nature of the flow sweeping the cold wall. For example, if no flow exists, ice nucleation is expected to occur early, whereas the presence of flow near the wall tends to delay the ice nucleation process. Since in the present problem the buoyancy-driven flow is seriously affected by the inclination angle, it is reasonable to expect that the ice nucleation time will also be dependent upon the inclination angle.

Figure 4a is a photograph of the flow field in the cavity for $\theta = 60^{\circ}$ and $t = 20$ min. Figure 4b presents a sketch of the flow field in Figure 4a, constructed based on our observations. It proved to be difficult to photograph the flow field, in particular near the ice interface. Based on Figures 4a and 4b, the flow in the liquid phase consists of a large counterclockwise rotating cell that fills most of the liquid region. Near the interface, a tall narrow clockwise rotating cell exists. This cell is created solely because of the presence of the density maximum of water at 4°C . Since the ice/water interface temperature is 0°C , the water in the close vicinity of the interface is lighter than the water at 4°C located a bit further but still close to the interface. Hence an upward-moving flow is created at the interface. The above description of the flow field is typical for most position angles about the vertical. At late times, as the temperature differences in the cavity diminish, the flow weakens significantly.

Temperature distributions at the centerline of the cavity perpendicular to the cold wall are shown in Figure 5. The symbols represent the experimental data and the lines the predictions of a simple theoretical model. No details of this model are presented here; they can be found in the literature.^{16,17}

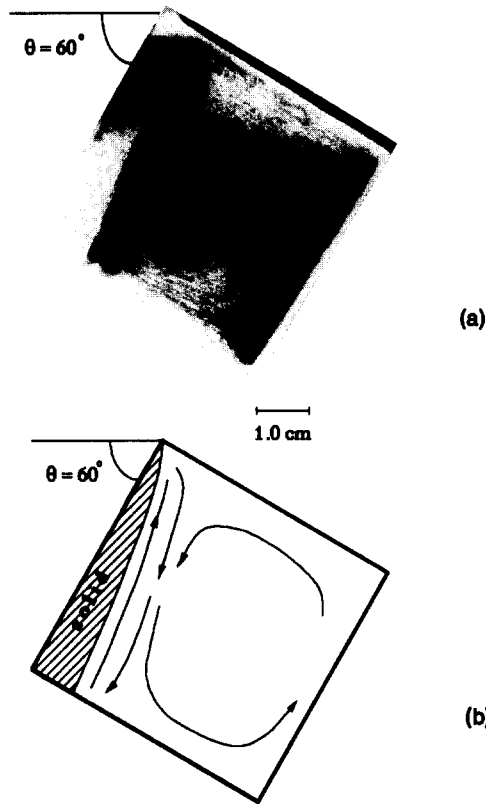


Figure 4 (a) Photograph of the flow pattern in the cavity for $\theta = 60^\circ$, $t = 20$ min; (b) schematic of the flow pattern for $\theta = 60^\circ$, $t = 20$ min

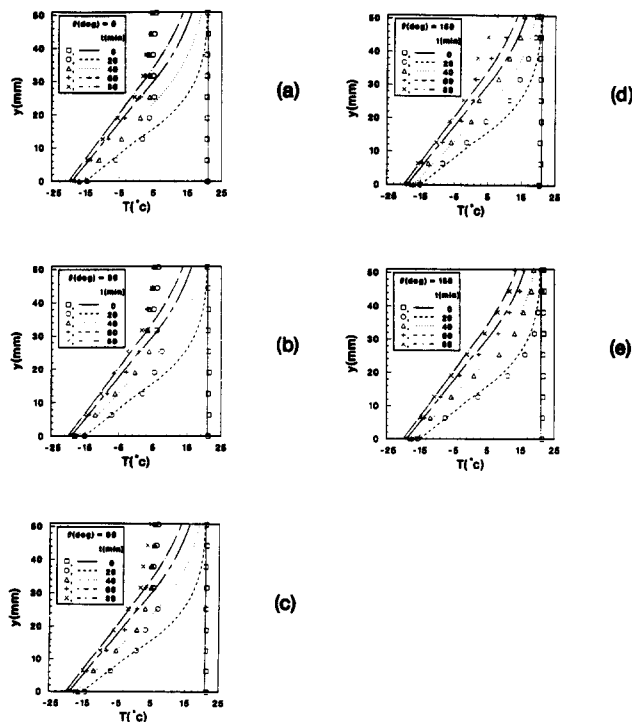


Figure 5 Temperature distribution at the centerline of the cavity. The symbols denote the experimental data and the lines the theoretical predictions

For clarity, however, the major assumptions contained in the model are reported: (a) the presence of the buoyancy-driven convection in the liquid phase is neglected; (b) the presence of the bottom wall is not taken into account, i.e., it is assumed that the liquid region is of infinite extent; and (c) the cold-wall temperature is assumed to be constant throughout the solidification phenomenon, and it is taken from the experimental data. The experiments indicate that in the cases where convection is expected to be strong ($\theta = 0^\circ, 30^\circ, 90^\circ$), the mixing caused by the flow is responsible for the fact that the temperature far from the interface and in the vicinity of the wall opposite to the cold wall becomes practically uniform in a relatively short time. As the angle changes to $\theta = 150^\circ$ and finally to $\theta = 180^\circ$ (where the cold wall is located on the underside), the temperature profiles indicate that heat conduction is the main heat transfer mechanism in the system.

In most cases, the temperature decreases monotonically as we move away from the cold wall. A notable exception to this fact are the early-time temperature distributions for $\theta = 30^\circ$ and $\theta = 90^\circ$, where convection is vivid in the liquid region. In these cases, the temperature increases as we move away from the interface, reaches a maximum, and decreases to a plateau thereafter.

The theoretical model performs well in predicting the temperature distribution in the ice (solid phase). On the other hand, the model does not perform well in predicting the temperature in the liquid phase when convection is important ($\theta = 0^\circ, 30^\circ, 90^\circ$), especially at early times when the driving temperature differences are large and the convection phenomenon is strong. As the temperature field becomes conduction dominated ($\theta = 150^\circ, 180^\circ$), the predictions of the theoretical model improve. The model performs best when $\theta = 180^\circ$. Note that even though in this case the cold wall is located on the underside, flow exists in the system and is caused by the partially unstable stratification initiated by the presence of the density extremum of water at 4°C . Unless the agreement between theory and experiment for $\theta = 180^\circ$ is fortuitous, this flow is not strong enough to alter the diffusion-dominated temperature distribution shown in Figure 5e. Certainly, as the temperature of water approaches 0°C , all convection in the system should cease.

Figures 6 and 7 present the main results on the growth of the ice/water interface. The interfaces in Figure 7 were traced by using photographs of the type shown in Figure 6. Clearly, the presence of natural convection severely carves the interface at early times (Figure 6, $t = 10$ min, 30 min; Figure 7a-e, $t = 15$ min, 30 min). As time increases and the temperature differences in the liquid region decrease through mixing, the flow weakens and the ice/water interface becomes flat and approximately parallel to the cold wall (Figure 6, $t = 50$ min, 70 min; Figure 7a-e, $t = 60$ min, 75 min). When the cold wall is situated at the top ($\theta = 0^\circ$), the flow in the cavity is bicellular and of the Bernard type. This is indicated by the shape of the interface and was verified by the flow visualization. As θ increases in the region $0^\circ < \theta \leq 120^\circ$ (Figures 6b-e), the flow gradually becomes what was described earlier in connection with Figure 6, and the interface shape at early times is dictated by the main counterclockwise rotating cell that fills most of the cavity. Increasing θ further to $\theta = 150^\circ$ and eventually to $\theta = 180^\circ$ retards the buoyancy-driven flow. The interface shape indicates that the solidification phenomenon at $\theta = 180^\circ$ in particular is diffusion dominated. Previous investigations of solidification of water around a pipe reported that the ice/water interface was not smooth and exhibited a groovelike structure along the spanwise direction.¹⁴ This structure was interpreted as the "footprint" of Bernard-Goertler instabilities on the ice/water interface. Such instabilities did not exist in our system, and the interface was rather plain and smooth. A typical flow pattern in our experiment was shown earlier in Figure 4.

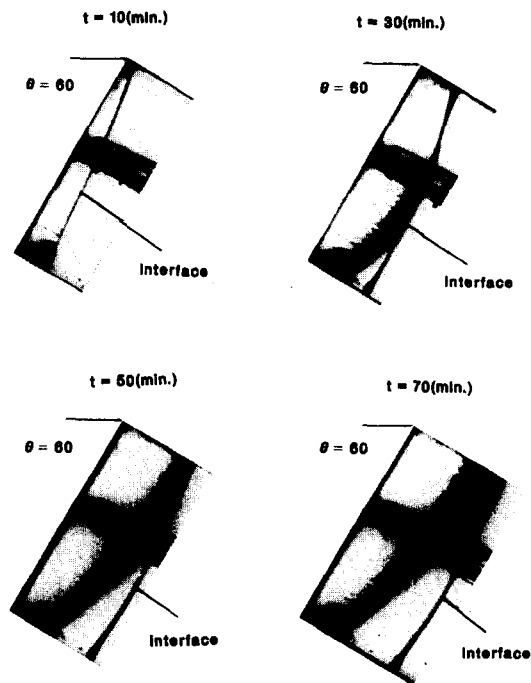


Figure 6 Sequence of photographs of the growth of the ice/water interface for $\theta = 60^\circ$

A result of engineering interest is the dependence of the volume of ice produced on time and on position angle. Figure 8 shows this result with the help of the dimensionless ice volume and time defined as

$$V^* = \frac{V}{V_T} \tag{1}$$

$$\tau = \frac{\alpha_s C_{ps} (T_i - T_0) t}{H^2 L} \tag{2}$$

While the ice volume increases monotonically with time for all angles, the dependence of the ice volume on the position angle is not as straightforward. Using a regression analysis¹⁸ for the data of Figure 8, the following correlation was obtained for the dependence of V^* on τ :

$$V^* = 3.515 \tau^{0.671} e^{-0.066 \cos(\theta - 41.92)} \tag{3}$$

The above correlation is plotted in Figure 9 together with all data points. It is felt that this correlation performs rather well in the region $0^\circ < \theta < 180^\circ$, $0^\circ < \tau < 0.08$ investigated in this study. A comparison between Equation 3 and published results for V^* from studies in which wax was used as the working substance was one of the suggestions of an anonymous reviewer of this article. After a literature search, we discovered that even though studies on water solidification exist for $\theta = 0^\circ$ or $\theta = 180^\circ$ in rectangular cavities, no correlations for V^* in the presence of convection are reported for the case of one cold and five adiabatic walls. The closest correlation we discovered was that of Ho and Viskanta⁷ for inward solidification in a rectangular cavity with conducting bottom and side walls and cooled from below ($\theta = 180^\circ$). In this study, solidification takes place because of *three* walls (the bottom wall and the two vertical side walls). The solid production rate is naturally expected to be higher than that of our study, in which cooling occurs through only one wall. Indeed, after the Ho and Viskanta⁷ correlation was compared to Equation 3 in Figure 9, it was found to overpredict the findings of the present study. This discrepancy, however,

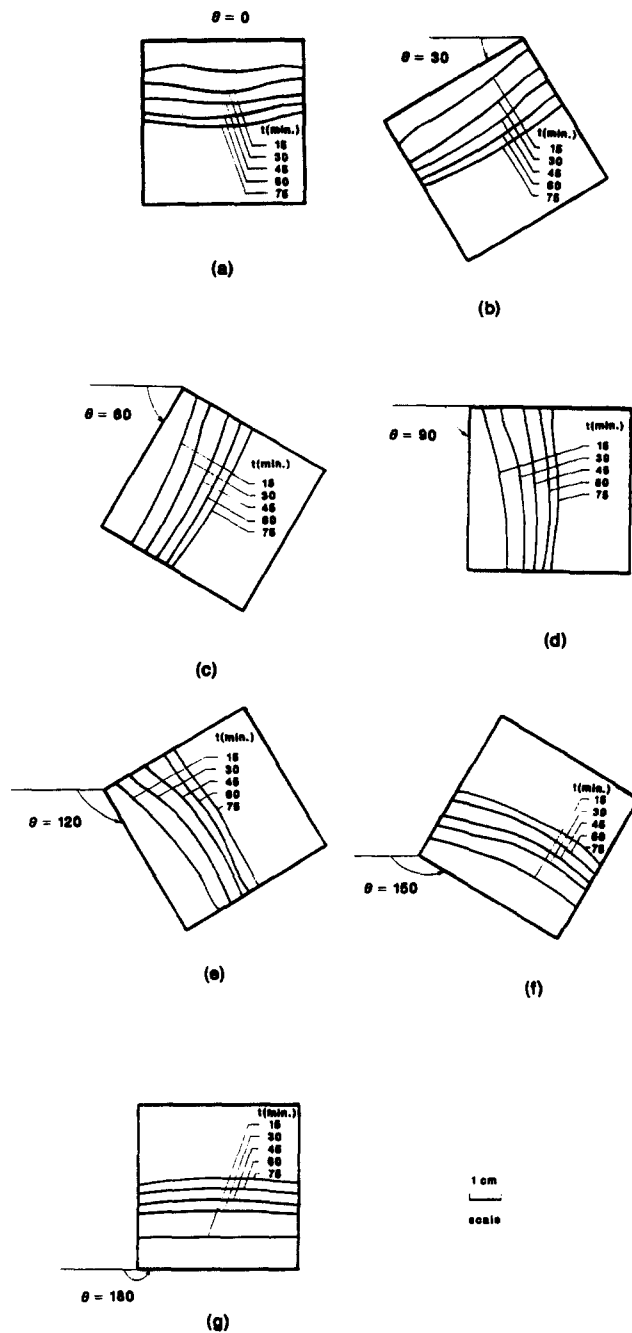


Figure 7 The growth of the ice/water interface for all inclination angles of interest

agrees with physical intuition based on the discussion outlined above describing the differences between our study and that of ref. 7.

Conclusions

An experimental study was performed for the problem of transient ice formation in a rectangular inclined cavity with one cold wall and five adiabatic walls. It was found that the temperature of the cold wall exhibits a jump at the time that ice first forms on its surface (ice nucleation time). The ice nucleation time reaches a maximum at an inclination angle of about 60° . After the initial ice formation, the wall temperature

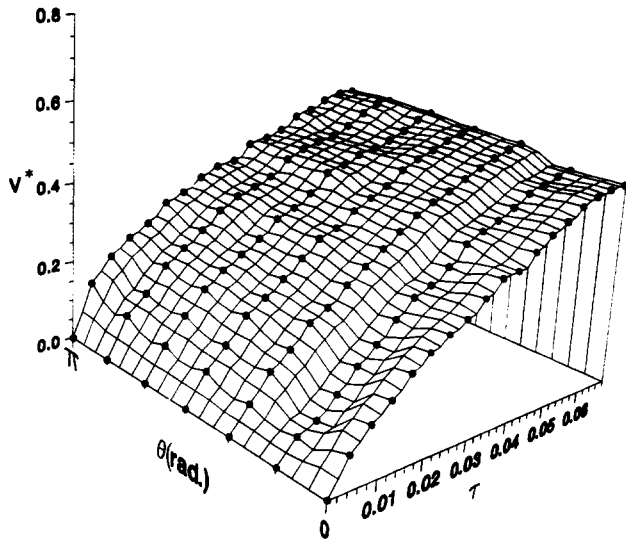


Figure 8 The dependence of the volume of ice formed on time and on the inclination angle

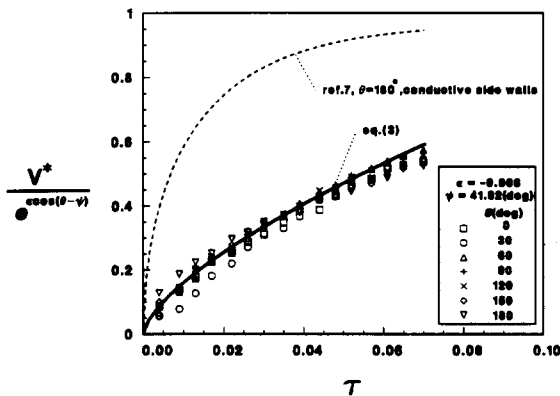


Figure 9 A comparison between Equation 3 and the data points for the volume of ice formed

decreases monotonically until a plateau is reached at large times.

Flow visualization indicated the existence of a large flow cell in the cavity rotating counterclockwise. An upflow at the ice interface caused by the presence of the density extremum of water at 4°C was responsible for the presence of a second long narrow cell rotating clockwise in the vicinity of the ice front. Detailed results on the temperature distribution in the cavity and the growth of the ice/water interface indicate that the presence of the natural convection severely affects the solidification phenomenon.

A simple theoretical model based on conduction predicted the temperature distribution in the ice region rather well. However, the model did not perform well in the liquid region when convection was vivid. The best agreement between the experiments and the theoretical model was observed at $\theta = 180^\circ$ where the system was, for the most part, stably stratified and

the only mechanism driving the flow was the presence of the density extremum of water at 4°C.

Detailed results on the dependence of the volume of ice formed in the system on time and on the inclination angle were reported. These results were summarized with the help of an engineering correlation (Equation 3).

Acknowledgments

Support for this work provided by NSF through grant no. ENG 84-51144 is gratefully acknowledged.

References

- 1 Viskanta, R. Natural convection effects in phase change heat transfer. *Natural Convection: Fundamentals and Applications* (S. Kakac et al., Ed.), Hemisphere, Washington, DC, 1985, 845-877
- 2 Boger, D. V. and Westwater, J. W. Effect of buoyancy on the melting and freezing process. *J. Heat Transfer*, 1967, **89**, 81-89
- 3 Diaz, L. and Viskanta, R. Visualization of the solid-liquid interface morphology formed by natural convection during melting of solid from below. *Int. Comm. Heat Mass Transfer*, 1984, **11**, 35-43
- 4 Hale, N. W. and Viskanta, R. Solid-liquid phase-change heat transfer and interface motion in materials cooled or heated from above or below. *Int. J. Heat Mass Transfer*, 1984, **23**, 283-292
- 5 Gau, C. and Viskanta, R. Flow visualization during solid-liquid phase change heat transfer I. Freezing in a rectangular cavity. *Int. Comm. Heat Mass Transfer*, 1983, **10**, 173-181
- 6 Gau, C. and Viskanta, R. Flow visualization during solid-liquid phase change heat transfer II. Melting in a rectangular cavity. *Int. Comm. Heat Mass Transfer*, 1983, **10**, 183-190
- 7 Ho, C.-J. and Viskanta, R. Inward solid-liquid phase-change heat transfer in a rectangular cavity with conducting vertical walls. *Int. J. Heat Mass Transfer*, 1984, **27**(7), 1055-1065
- 8 Webb, B. W. and Viskanta, R. Natural-convection-dominated melting heat transfer in an inclined rectangular enclosure. *Int. J. Heat Mass Transfer*, 1986, **29**(2), 183-192
- 9 Van Buren, P. D. and Viskanta, R. Interferometric observation of natural convection during freezing from a vertical flat plate. *J. Heat Transfer*, 1980, **102**, 375-378
- 10 Jany, P. and Bejan, A. Scaling theory of melting with natural convection in an enclosure. *Int. J. Heat Mass Transfer*, 1988, **31**(6), 1221-1235
- 11 Cheng, K. C., Inaba, H., and Gilpin, R. R. Effect of natural convection on ice formation around an isothermally cooled horizontal cylinder. *J. Heat Transfer*, 1988, **110**, 931-937
- 12 Gilpin, R. R. Cooling of a horizontal cylinder of water through its maximum density point at 4°C. *Int. J. Heat Mass Transfer*, 1975, **18**, 1307-1315
- 13 Gilpin, R. R. The effects of dendritic ice formation in water pipes. *Int. J. Heat Mass Transfer*, 1977, **20**, 693-699
- 14 Hermann, J., Leidenfrost, W., and Viskanta, R. Effect of natural convection on freezing of water around an isothermal horizontal cylinder. *Int. Comm. Heat Mass Transfer*, 1984, **11**, 301-310
- 15 Sadowski, D., Poulikakos, D., and Kazmierczak, M. Three dimensional natural convection experiments in an enclosure. *AIAA J. Thermophysics Heat Transfer*, 1988, **2**, 242-249
- 16 Carslaw, H. S. and Jaeger, J. C. *Conduction of Heat in Solids*, 2nd ed., Oxford University Press, New York, 1959
- 17 Ozisik, M. N. *Heat Conduction*, Wiley, New York, 1980
- 18 Draper, N. R. and Smith, H. *Applied Regression Analysis*, 2nd ed., John Wiley & Sons, New York, 1981